32-channel 100-GHz-spaced demultiplexer for metropolitan area networks

Jie Qiao
Feng Zhao
Microelectronics Research Center
Department of Electrical and Computer Engineering
University of Texas at Austin
Austin, Texas 78758

James W. Horwitz
Radiant Photonics Inc.
Braker "B"
1908 Krama Lane
Austin, Texas 78758

Ray T. Chen
Microelectronics Research Center
Department of Electrical and Computer Engineering
University of Texas at Austin
Austin, Texas 78758
E-mail: raychen@uts.cc.utexas.edu

Abstract. We report a high-density wavelength division demultiplexer (Demux) capable of demultiplexing a 32-channel 100-GHz-spaced wavelength, with a working wavelength range of operation from 1541.37 to 1565.47 nm. The design, packaging, and performance of the Demux using the 22nd diffraction order of an echelle grating is described. The typical insertion loss of the device is -3.0 ± 0.2 dB, the cross talk between adjacent channels for all 32 channels is about -30 dB, and the average 1-dB optical passband is 0.256 nm. We found the experimental measurement result of the 1-dB passband to be in good agreement with the theoretical 1-dB passband as calculated. The device has single-mode fiber in and multimode fiber out, and thus can bridge the telecommunication backbone and local area networks. [DOI: 10.1117/1.1385333]

Subject terms: Wavelength division demultiplexer; echelle grating; dispersion ability; DWDM packaging.

Paper 200319 received Aug. 11, 2000; revised manuscript received Feb. 6, 2001; accepted for publication Feb. 9, 2001.

1 Introduction

Rapid growth in demand for high-capacity telecommunication links, in the context of the speed limitation of single-wavelength links, has generated worldwide interest in dense wavelength division demultiplexers[1] (demuxes) as an effective higher-capacity solution for optical networks. Several major technologies for making demuxes include interference filters, Bragg grating filters, and phased-array-based demuxes.[2–6] Technologies using interference filters and Bragg grating filters[7] reach a low level of fiber-to-fiber loss, but the losses are not uniform across the whole wavelength range. Interference filters and Bragg grating filters use discrete components, so that increasing the number of channels proportionately increases the cost and the packaging volume. Interference filters entail multicavity structures requiring tens of tightly controlled dielectric layers in order to produce individual filters. It is difficult by this means to fabricate devices with channel spacing less than 100 GHz. Phasars and etched gratings[7] have good and uniform insertion losses, but may not have satisfactory temperature control and polarization sensitivity, depending on the composite materials.

In this paper, we discuss a 32-channel 100-GHz DWDM based on an echelle grating. It shows equalized insertion losses of -3.0 ± 0.2 dB within all the channels, and offers considerable benefit to the cost and power budgets. We include a discussion of DWDM design, packaging, and performance data.

2 DWDM Structure and Optical Design

Figure 1 is a schematic of the device design and packaging. Thirty-two channel wavelength division multiplexer (WDM) wavelengths are introduced into the DWDM device by a single-mode fiber with an FC connector, and then are collimated by a multielement lens. The same lens functions as the focusing lens for the demultiplexed signals. We used an echelle grating to demultiplex 32 optical signals within the C band with 100-GHz channel spacing. The working wavelength range of operation is from 1541.37 to 1565.47 nm. A grating with 78.85% diffraction efficiency for both the TE and TM modes at a center wavelength of 1554.94 nm diffracts the incident light beams into different directions. The ITU fiber optic telecommunication channel standard[8,9] determines the wavelength choice. In order to eliminate multiple alignment for individual fibers and increase throughput, we employed a 32-channel silicon V-grooved fiber array to receive the 32 demultiplexed signals. The output fiber array sits right on the top of the input fiber array, which only has a single fiber. The input fiber is aligned with the center of output fiber array. We call this kind of structure an over-under configuration. The core size of the multimode glass fiber is 62.5 μm. This DWDM device is designed for optical communications for metropolitan-area networks where free-space DWDM and multimode fiber band networks are jointly employed.[10]

Several journal articles have proposed DWDM with different optical configurations.[2,3] A high-order echelle grating has several special properties that make it an excellent diffraction component for WDM diffraction. Most apparent is its high dispersion, which permits compact optical systems with a high throughput and high resolution. In addition, because it is never used far from the blaze direction, the grating's efficiency remains relatively high over a large spectral range. Furthermore, when the grating is operated at higher orders, it is nearly free of the polarization effect.[11]

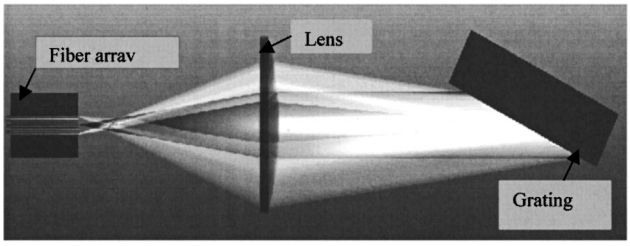

Fig. 1 Geometrical layout of a 100-GHz-spaced 32-channel demultiplexer, with a packaging size of 157×61×38 mm.

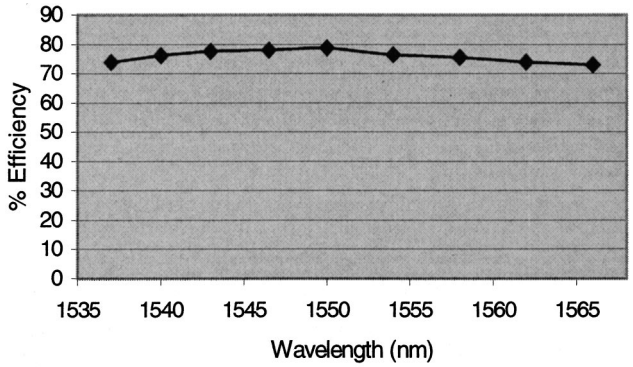

Fig. 2 Measured grating efficiency versus wavelength.

Under the Littow mount condition, when the incident angle is the same as the diffraction angle, another useful property comes into play: one lens can collimate and focus simultaneously, resulting in lower cost and decreased packaging size for the WDM system.

Usually, the higher the grating order, the smaller the polarization effect of the grating. But any given grating order is also limited by certain factors. One of them is its working spectral range. We calculated the corresponding grating working order to cover the C-band spectral range (from 1528 to 1560 nm). When the extremes of the C band are $\lambda_1 = 1528$ nm and $\lambda_2 = 1560$ nm, the formula for calculating the grating order for a certain spectral range can be expressed as[11]

$$m = \frac{\lambda_1}{\lambda_2 - \lambda_1}. \tag{1}$$

So that the spectrum of the C-band signal λ_2 operating at order m does not overlap the spectrum of the signal λ_1 when operating at order $m+1$, m must be less than 47. On the other hand, we must leave room to fully reduce the noise caused by the scattering of adjacent orders. We chose 22 as the grating working order, under which the grating is almost free of the polarization effect.

The reflection-grating diffraction equation is[12]

$$d(\sin\theta_i + \sin\theta_d) = m\lambda, \tag{2}$$

where m is the order of diffraction, λ the wavelength, d the groove spacing, and θ_i and θ_d the angles of incidence and diffraction. We found the angular dispersion by taking the first derivative of θ_d:

$$\frac{d\theta_d}{d\lambda} = \frac{\sin\theta_i + \sin\theta_d}{\lambda\cos\theta_d}. \tag{3}$$

For the Littrow condition $\theta_i = \theta_d$, angular dispersion is

$$\frac{d\theta_d}{d\lambda} = \frac{2\tan\theta_d}{\lambda}. \tag{4}$$

The larger the diffraction angle, the greater the angular dispersion. In our design of the 32-channel demux, taking into consideration the trade-off between angular dispersion and its linearity,[13] we chose incident and diffraction angles of $\theta_i = \theta_d = 64.1$ deg at the center wavelength of 1554.94 nm, which is the 18th channel of our device. The angular dispersion of the grating at the central wavelength ($\lambda = 1554.94$ nm) is 0.152 deg/nm (2.64 mrad/nm).

Figure 2 shows our measurements of the grating efficiency across all working wavelengths. The grating efficiency varies from 70% to 78.85% over the whole range. The efficiency peak occurs at a wavelength of 1554.94 nm, the center wavelength, employing the 22nd diffraction order of the grating. The 18th channel receives this wavelength and is thus defined as the center channel. The following equation determines the channel spacing between a given channel and the central channel:

$$\Delta d = f\tan(\theta_d - \theta_{dc}), \tag{5}$$

where f is the focal length; θ_{dc} is the diffraction angle at the center wavelength, which equals the incident angle; and θ_d is the diffraction angle of the specific channel under evaluation.

3 Demultiplexer Packaging and Performance

We used active alignment in the assembling procedure. It is critical to locate the focal point of the lens and to set the input fiber array exactly at the focal plane. We used a stage with five degrees of freedom to actively align the grating. We found the position of highest diffraction efficiency for the grating by fine-tuning the rotation and the pitch of the grating. To arrive at its highest and most balanced coupling efficiency, we simultaneously monitored the output of the two edge channels and the center channel, i.e., the 1st channel, the 18th channel, and the 32nd channel, at wavelengths of 1541.37, 1554.93, and 1564.47 nm, respectively. In this way the alignments for other channels can be optimized automatically.

Figure 3 shows the output spectrum of the 32-channel DWDM. It indicates that the output signals of the 32 channels are quite uniform. The output spectrum was measured with a laser rather than a wideband white light source, so it shows the center wavelength of each individual channel rather than the exact loss spectrum, because of the narrow linewidth of the laser.

The *insertion loss* is defined as the difference between the input power of the DWDM device and the output power via the silicon V-grooved fiber array. This loss includes the loss in the input single-mode fiber, lens, grating, silicon V-grooved fiber array, and connectors, and the coupling loss from free space to output fiber array. The *adjacent-*

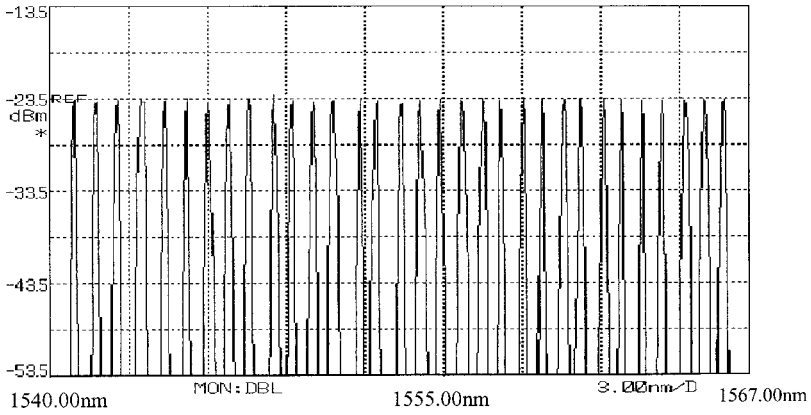

Fig. 3 The output spectrum of the 32-channel demux.

channel cross talk is the power ratio between a specific channel and its adjacent channels when only the specific channel is activated. Figure 4 shows the measurement of insertion loss for all 32 channels, which is also quite uniform across channels. Our measurements show the typical insertion loss of this WDM system to be -3.0 ± 0.2 dB. Of the 3.0 dB, 1.3 dB is due to the fact that the grating diffracts only 74.4% of the incident power into the desired diffraction order. Transmission and reflection loss of the lens accounts for 0.3 dB. The remaining 1.4 dB is caused by lens aberration and misalignment. The adjacent-channel cross talk is in the neighborhood of -30 dB for all 32 channels.

By tuning the wavelength of a specific channel when all the channels are aligned, we found the average 1-dB optical passband of the 32 channels to be 0.256 nm. Figure 5 shows the 1-dB optical passbands of all channels. The passbands vary from 0.22 to 0.31 nm, because the quality of the output light spot varies at different channels. The average value of the 1-dB passband is 0.256 nm. Because WDM laser sources usually contain a spectral width that depends on the laser cavity structures and on operating conditions, a laser wavelength shift is also present when the laser is internally modulated.[14] The relatively large 1-dB optical passband makes our demux robust to the disturbance caused by laser wavelength shift. When all the channels are aligned and minimum insertion losses are achieved, the output fiber array is moved laterally in 2-μm steps to the left and to the right side of a specific channel until the insertion loss increases by 1 dB. We measured the 1-dB passband of all channels as a function of lateral misalignment. The experiment supports the conclusion that the WDM system can tolerate lateral misalignment up to 30 μm while maintaining a better than 0.256-nm 1-dB passband for all 32 channels.

Figure 6 shows the measurement of the 1-dB physical passband for channel 32, corresponding to 30-μm lateral misalignment. This large dynamic range makes the device highly robust against any displacement of output fiber array caused by misalignment, temperature fluctuation, or vibration. Employing a specially made single-mode fiber array, and thereby decreasing the fiber-to-fiber spacing by half, we were able to use the same configuration to realize a 64-channel DWDM with 50-GHz spacing.

4 Simulation for Image Shift Tolerance within the 1-db Passband

Disturbances caused by laser drift, temperature change, and vibration are reflected as a relative movement of the input light spot at the receiving fiber or as a shift of wavelength. A larger 1-dB passband is therefore always preferable. The larger the ratio of the core diameter to the distance between the receiving fibers, the larger the 1-dB passband.[15]

To calculate the transverse loss, suppose the core diameter of the receiving fiber to be $D=2R$, and the diameter of the input light spot to be $d=2r$. We express the ratio of energy in the area of overlap (input light spot and receiving fiber) to energy in the entire area of the input light spot as

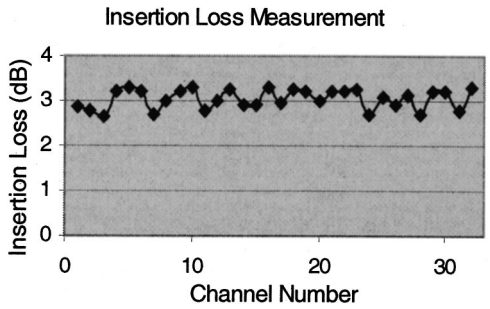

Fig. 4 Experimental result of measuring the insertion loss for all 32 channels.

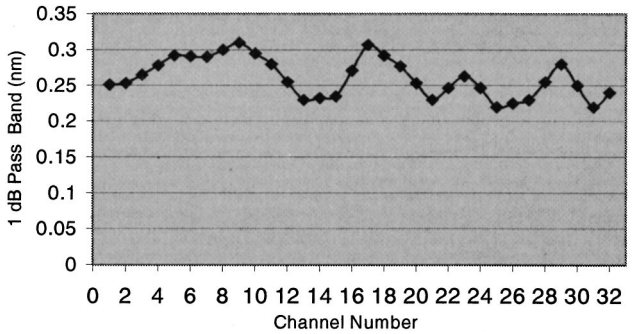

Fig. 5 Measured 1-dB optical passband for all 32 channels.

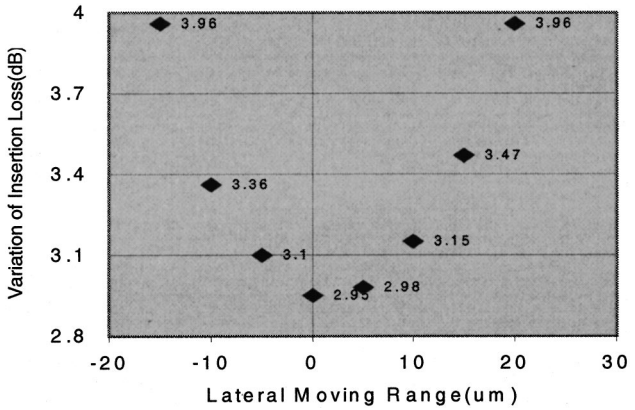

Fig. 6 Measured 1-dB physical passband for channel 32. When lateral movement reaches 15 μm to the left or 20 μm to the right of the center channel 32, insertion loss increases by 1 dB.

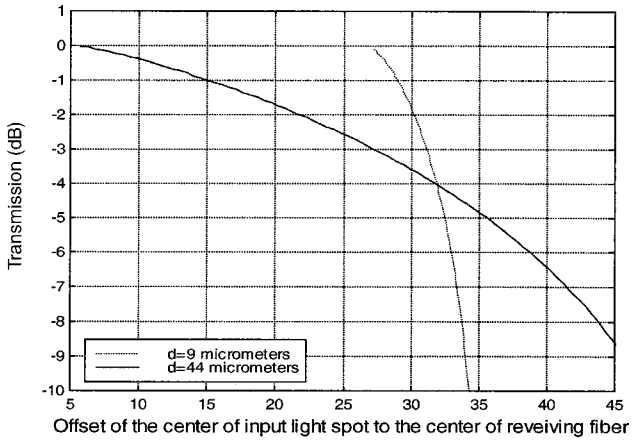

Fig. 8 Simulation result of transverse loss versus offset of fiber cores with different transmitting spot sizes.

$$\eta = \frac{\int_{s'} f'(x,y)\, ds'}{\int_{s} f(x,y)\, ds}, \tag{6}$$

where η is the energy ratio, s' is the overlap area, s is the input light spot area, and $f'(x,y), f(x,y)$ are the optical power distribution function in the overlap area and the whole area of the input light spot, respectively. Figure 7 illustrates Eq. (6). The wavelength shift of a specific channel causes the image of the input light spot to move accordingly. We can thus obtain the maximum movement tolerance of the WDM system when operating within 1-dB passband range.

Here, we assume a uniform power distribution across the whole area of the input light spot. We set up two simulations for the theoretical 1-dB passband calculation, in which $D = 62.5\ \mu$m. In one case, $d = 9\ \mu$m, the core diameter of the single-mode fiber. In the other, $d = 44\ \mu$m. Figure 8 shows the simulation result, which indicates that when a system is diffraction-limited, i.e., the input spot size is the same as the single-mode fiber core diameter, the maximum lateral movement tolerance can be up to $\pm 29\ \mu$m within the 1-dB passband.

5 Discussion

An average of $\pm 15\ \mu$m of lateral movement tolerance was shown in our experiment, a result that agrees with $d = 44\ \mu$m, which represents the worst spot quality we found in our lens design simulation. The lens used in our WDM system is a two-element lens. We can certainly achieve larger lateral movement tolerance by using more elements to obtain a diffraction-limited system.

To evaluate the nonlinearity performance of the device when working at ITU standard wavelengths, by combining Eqs. (2) and (3) we can simulate the relation between angular dispersion and wavelength. The result is shown in Fig. 9. The 32-channel designation on the x axis of the figure corresponds to the 32 wavelengths, which are determined by the ITU grid. We found that the angular dispersion increases when the wavelength increases and that therefore the channel spacing depends on wavelength. Figure 10 shows the simulated channel spacing of 32 wavelengths, which fit exactly within the ITU grid. We found the channel spacing to vary from 115 to 135 μm across all 32 channels. When building the 32-channel prototype demux, we tuned the individual wavelengths slightly to eliminate the nonlinear effect of angular dispersion. We found we could make the wavelengths fit exactly within the ITU grid by using a nonlinearly spaced V-grooved fiber array.

6 Conclusions

We built and tested a fully packaged 32-channel 100-GHz demux. The insertion losses of all 32 channels are within -3.0 ± 0.2 dB. The cross talk between adjacent channels for all channels is close to -30 dB. The average 1-dB

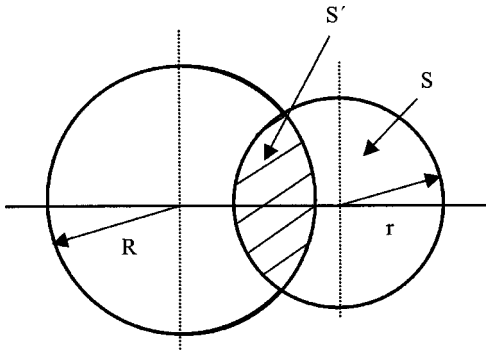

Fig. 7 Illustration of the region of overlap for offset fiber cores.

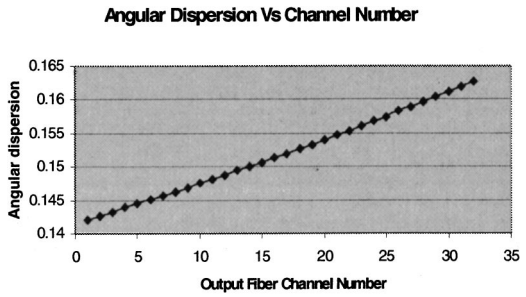

Fig. 9 Angular dispersion at different wavelengths. The larger the wavelength, the greater the angular dispersion.

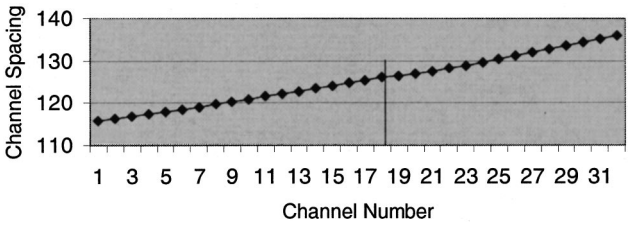

Fig. 10 Illustration of unequal channel spacing caused by dependence of wavelength on angular dispersion.

optical passband is 0.256 nm, which makes the device robust to disturbances caused by wavelength and temperature fluctuations. A 64-channel DWDM with 50-GHz spacing accuracy is feasible using the same configuration while decreasing the fiber-to-fiber spacing by half.

Acknowledgments

This research is currently supported by the Ballistic Missile Defense Organization, DARPA, AFOSR, the 3M Foundation, and the Advanced Technology Program (ATP) of the State of Texas. The authors thank their colleague Wei Jiang for a valuable discussion.

References

1. J. P. Laude, *Wavelength Division Multiplexing*, Prentice-Hall (1993).
2. L. H. Spiekman, M. R. Amersfoort, A. H. de Breede, F. P. G. M. van Ham, A. Kuntze, J. W. Pedersen, P. Demeester, and M. K. Smit, ''Design and realization of polarization-independent phased array wavelength demultiplexers,'' *J. Lightwave Technol.* **14**, 991 (1996).
3. M. K. Smit and C. van Dam, ''PHASAR-based WDM devices: principles, design and applications,'' *IEEE J. Sel. Top. Quantum Electron.* **2**, 236 (1996).
4. S. M. Ojha, G. H. B. Thompson, C. G. Cureton, C. B. Rogers, S. J. Clements, M. Asghari, and I. H. White, ''Demonstration of low loss integrated InGaAsP/InP demultiplexer device with low polarization sensitivity,'' *Electron. Lett.* **29**, 905–907 (1993).
5. M. R. Amersfoort, C. R. de Boer, B. H. Berbeek, P. Demeester, A. Looyen, and J. J. G. M. van der Tol, ''Low loss phased-array based 4-channel wavelength demultiplexer integrated with photodetectors,'' *IEEE Photonics Technol. Lett.* **6**, 62–64 (1994).
6. R. Mestric, H. Bissessur, B. Martin, and A. Pinquier, ''1.31–1.55 μm phased array demultiplexer on InP,'' *IEEE Photonics Technol. Lett.* **8**, 638–640 (1996).
7. E. S. Koteles, ''Integrated planar waveguide demultiplexers for high density WDM application,'' in *Wavelength Division Multiplexing*, R. T. Chen and L. S. Lome, Eds., pp. 3–32, SPIE Press (1999).
8. Telecommunication Standardization Sector of the International Telecommunication Union (ITU-T), Geneva, http://www.itu.ch.
9. A. McGuire and P. Bonenfant, ''Standards: the blueprint for optical networking,'' *IEEE Commun. Mag.* **36**, 68–75 (1998).
10. T. Niewulis, ''Accessible fiber to the last mile,'' presented at Symp. on Optical Internet, January 18–20, 2000, Dallas.
11. M. C. Hutley, *Diffraction Gratings*, p. 35, Academic Press (1982).
12. E. G. Loewen and E. Popov, *Diffraction Gratings and Applications*.
13. J. Qiao, F. Zhao, J. Liu, and R. T. Chen, ''Dispersion-enhanced volume hologram for dense wavelength-division demultiplexer,'' *IEEE Photonics Technol. Lett.* **12**, (2000).
14. P. Bhattacharya, *Semiconductor Optoelectronic Devices*, p. 323, Prentice-Hall (1994).
15. J. Hirsh, V. Y. Kalindjian, F. S. Lin, M. R. Wang, G. Xu, and T. Jannson, ''High channel density broadband wavelength division multiplexers based on periodic grating structures,'' *Proc. SPIE* **2532**, 171–181 (1995).

Jie Qiao received her MS from the Department of Precision Instruments, Tsinghua University, China, in 1997. She is now a PhD candidate in the Department of Electrical and Computer Engineering at the University of Texas at Austin. Her research fields include dense and coarse wavelength division demultiplexing, optical networks, fiber optics, optical interconnects, and optical communications.

Feng Zhao received his PhD in optics in 1991 from Harbin Institute of Technology in China. He is a research fellow at the Microelectronics Research Center of the University of Texas at Austin. He has published more than forty papers. His research fields include WDM, optical interconnects, fiber optic, optical communications, optical networks, optical storage, optical information processing, and laser and nonlinear optics.

James W. Horwitz earned a BS degree in chemistry from Rutgers College in 1963 and an MS degree in physics from New York University in 1971. He took graduate courses in optics at the University of Rochester. In 1964 he joined Perkin-Elmer Corporation, where he worked on the development of gas sensors utilizing absorption of infrared and vacuum-ultraviolet radiation. He later joined EDO/Barnes Engineering, where he worked with infrared radiometers and designed lenses. He became interested in the optical design of spectrometers, wrote a computer program for this purpose, and published a paper on this subject. Subsequently, he became involved in writing several optical design programs and led the development of an 11,000-line program that did ray tracing and radiometric analysis. In the 1970s and 1980s he was with Tropel Corporation, Bausch & Lomb, and Mendon Research Corporation. He worked on MTF analyzers, Twyman-Green interferometers, and the design of microscopes, and helped develop an automated eye refractor. He has been with Radiant Photonics since 1999, where he leads the optical engineering effort for wavelength-division multiplexers and related equipment. At Radiant Photonics, he has designed the optics for numerous such systems. He is a member of the OSA, a past member of SPIE, and an officer of the Central Texas Society for Optics.